INFLUENCE OF SHOT PEENING ON THE MICROSTRUCTURE AND THE BENDING FATIGUE STRENGTH OF BAINITIC-AUSTENITIC NODULAR CAST IRON

A. Ebenau, D. Löhe, O. Vöhringer and E. Macherauch,
Institut für Werkstoffkunde I, Universität Karlsruhe, D-7500 Karlsruhe, FRG

ABSTRACT

Bainitic-austenitic nodular cast iron, which is produced by austenitizing and incomplete isothermal transformation, shows high tensile strength combined with remarkable ductility. In the present paper, the consequences of shot peening on the surface and subsurface material states and on the bending fatigue behaviour are investigated. Pearlitic nodular cast iron was austempered in a salt bath at 300 ^{o}C (type A) and 380 ^{o}C (type B). Type A contains about 22 vol.-% retained austenite and type B about 39 vol.-%. By shot peening, characteristic depth distributions of residual stresses, half width of X-ray interference lines, retained austenite and microhardness are produced. In both material states, a strong peening induced transformation of retained austenite into martensite appears. Therefore the depth distributions of compressive residual stresses show two maxima: the first below the surface and the second directly at the surface. This phenomenon can be explained by the volume increase as a consequence of peening induced transformation of retained austenite into martensite.

The increase of fatigue life and fatigue limit by shot peening is much more significant for type B (115 %) than for type A (31 %). In both cases, the crack initiation site is shifted below the surface. The results obtained cannot be understood on the basis of the local fatigue strength concept alone, which takes into consideration of the peening induced alterations of residual stresses and hardness. It is assumed that the high fatigue strength of shot peened material of type B is caused by a much higher resistance against crack initiation below the surface than at the surface. The underlying mechanism is a strong workhardening and strain assisted transformation of retained austenite into martensite, which locally produces large hydrostatic stress components retarding the spreading and the coalescence of microcracks present in the investigated material states already after the first cycle.

KEYWORDS

Nodular cast iron, austempering, bainite, retained austenite, bending fatigue strength, fatigue life, fatigue limit, transformation of retained austenite into martensite, strain assisted transformation, decohesions, microcrack nucleation, crack propagation.

INTRODUCTION

Austempered nodular cast irons are interesting materials for highly stressed castings because they combine high strength with remarkable ductility [1-3]. Their microstructure, which strongly depends on the isothermal transformation temperature, is composed of graphite, bainitic ferrite, retained austenite and eventually (after transfomation at relatively low temperatures) carbide. The volume fraction of retained austenite depends on temperature and duration of the austempering treatment and may come to 40 %. The stress and/or strain assisted transformation of retained austenite to martensite, which locally changes the microstructure and the stress state, is an important phenomenon regarding the mechanical behaviour of austempered nodular cast iron subjected to quasistatic or cyclic loading. On the other hand, transformation of retained austenite may occur during machining or peening of castings or specimens, thereby changing the microstructure and the residual stress state near the surface and consequently also the fatigue properties. Therefore, it is not surprising that fatigue limits of austempered nodular cast irons given in the literature show large scattering even if similar chemical compositions and heat treatments are compared [1,4-6].

In the present report, the influence of shot peening on the surface and subsurface material state of nodular cast iron, austempered at 300 and 380 °C, is investigated. The depth distributions of residual stresses, the half width of X-ray interference lines, the microhardness and the volume fraction of retained austenite are determined. Then, the influence of shot peening on the fatigue strength of both heat treating states is quantitatively determined and discussed. Special attention is paid to the influence of retained austenite and its transformation by shot peening and subsequent cyclic loading.

EXPERIMENTAL PROCEDURE

The chemical composition of the material investigated was 3.5 C, 2.75 Si, 0.41 Mn, 0.6 Cu, 0.06 Ni, 0.03 Mo, 0.028 P, 0.003 S and less than 0.005 Cr (mean values in weight percent). The as cast microstructure was mainly pearlitic containing about 25 vol.-% "bulls eye" ferrite. From the Y2 keel blocks, flat bending fatigue specimens of 2.2 mm thickness were machined. These specimens were austenitized 30 min at 900 °C in a fluidized bed and austempered in a salt bath 2 hours at 300 °C (type A) and 380 °C (type B), respectively. The heat treatments, the volume fraction of retained austenite (RA), the hardness (HV 10), the 0.2 % proof stress ($R_{p0.2}$), the ultimate tensile strength (R_m) and the elongation after fracture (A_5) are summarized in Table 1.

Tab. 1 Heat Treatment, Volume Fraction of Retained Austenite and Mechanical Properties of Material States Investigated

type	Austempering temp. [°C]/time [h]		RA [vol.-%]	HV 10	$R_{p0.2}$ [N/mm²]	R_m [N/mm²]	A_5 [%]
A	300	2	22	500	1226	1498	8.0
B	380	2	39	360	848	1038	3.8

The microstructure of type A is composed of very fine lower bainite, retained austenite and some martensite. The microstructure of type B is coarser containing upper bainite and retained austenite which is more homogeneously distributed than in type A.

After the heat treatment, the specimens were ground to a final thickness of 2 mm. One half of the specimens was shot peened in a Baiker air blast machine. A cast steel shot S 330 with a hardness ranging from 54 to 58 HRC was used. In the case of material A, the peening pressure was 5 bar and the coverage 5 · 98 %. Type B was peened with 3 bar until a coverage of 3 · 98 % was achieved.

Depth distributions of residual stresses were determined by X-ray measurements according to the $\sin^2\psi$-method [7]. The {211}-interference lines of the bcc phases bainitic ferrite and martensite were evaluated using $CrK\alpha_1$-irradiation. As a measure of workhardening and micro residual stresses, respectively, the half width of the X-ray interference lines were determined at ψ-angles of -9^o, 0^o and $+9^o$. The volume fraction of retained austenite was also determined by X-rays, using $MoK\alpha_1$-irradiation. The evaluation was carried out according to the 5-lines procedure [8].

Deflection controlled bending fatigue tests were run on electromechanical bending fatigue machines, type Schenk PWO. The load versus time dependence was sinusoidal, the frequency amounts to 25 Hz. The tests were run to an ultimate number of cycles of 10^7, unless fracture intervened. The evaluation of the bending fatigue tests was carried out according to the arcsin $\sqrt{p}$ procedure [9].

EXPERIMENTAL RESULTS

The depth distributions of residual stresses after shot peening of both material states are given in Fig. 1. In material state A, the peening induced compressive residual stresses

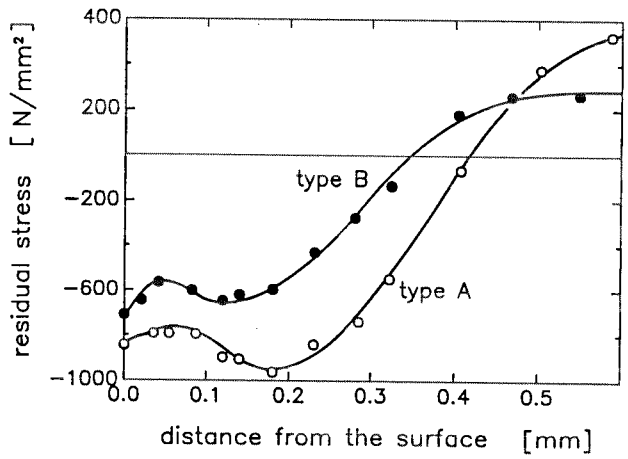

Fig. 1 Residual stress as a function of distance from surface

have larger amounts and extend to a greater depth than in type B. In both cases, there are two maxima of compressive residual stresses: One in the direct surface and another 0.18 mm (type A) or 0.12 mm (type B) below the surface.

In Fig. 2, the depth distribution of half width of the X-ray interference lines are shown. The values obtained from material state A are always larger than those from material state B. In both cases, a maximum at the surface and a miminum 0.18 mm below the surface are observed. In material state A, shot peening causes a marked reduction of

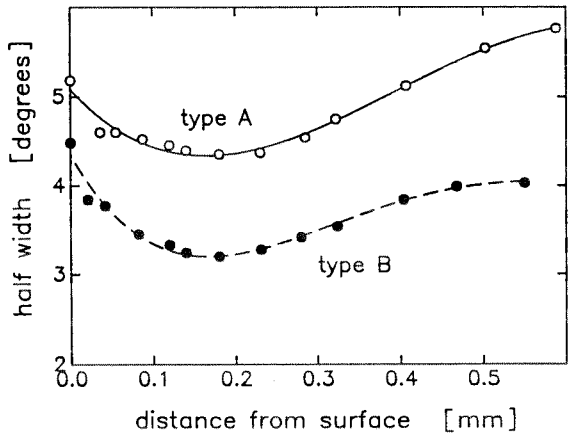

Fig. 2 Half width of X-ray interference lines as a function of distance from surface

measured values compared to the bulk material for which the largest values are determined. In material state B, the peening induced variation of half width is less pronounced. In the vicinity of the surface, larger values are measured than in the bulk material.

The depth distribution of low load hardness HV 0.5 measured in type A and B are given in Fig. 3. In both material states, the hardness continuously decreases from the surface to

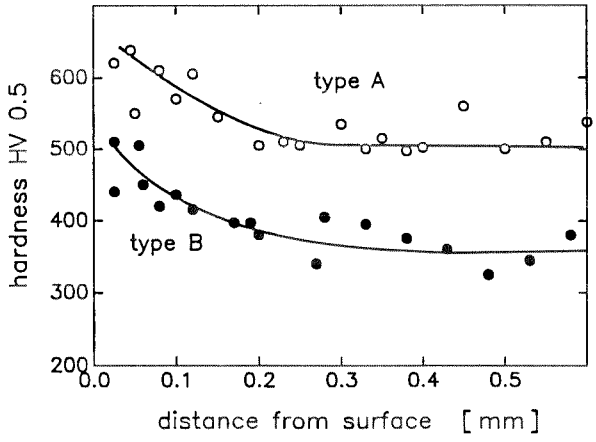

Fig. 3 Hardness HV 0.5 as a function of distance from surface

the interior of the specimens investigated. Fig. 4 shows the volume fraction of retained austenite measured after shot peening as a function of the distance from surface. At the surface of both material states, the content of retained austenite is rather low. With increasing distance from surface, the measured values increase towards the level of unpeened specimens. Peening induced transformation of retained austenite occurs to a depth of 0.3 mm (type A) and 0.2 mm (type B), respectively.

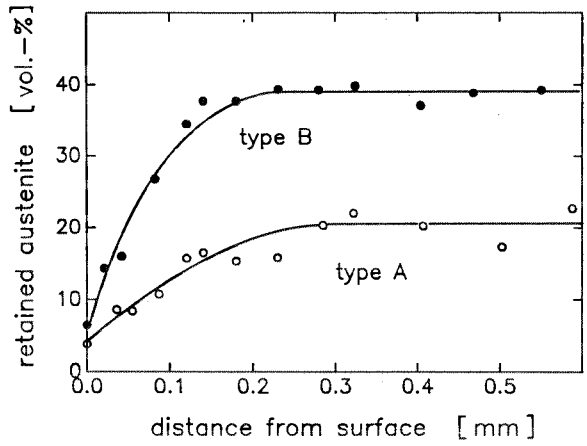

Fig. 4 Retained austenite as a function of distance from surface

The results of the bending fatigue tests are shown in Fig. 5. In the unpeened condition, the fatigue limits of type A (295 N/mm^2) and type B (260 N/mm^2) do not differ much. Crack initiation always occurs at the surface of the specimens. By shot peening, the

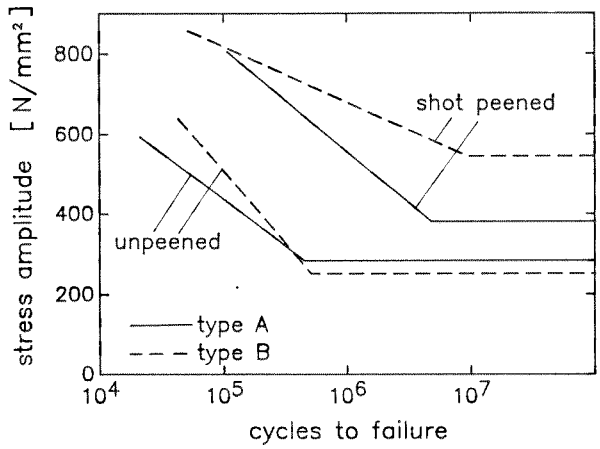

Fig. 5 SN-curves of cyclic bending testes of bainitic-austenitic nodular cast iron in unpeened and shot peened conditions

fatigue limit is increased to 385 N/mm^2 (type A) and 560 N/mm^2 (type B), respectively. The increment of material state B (115 %) is much larger than that of material state A (31 %). Crack initiation was always observed below the surface, even at stress amplitudes as high as 800 N/mm^2.

DISCUSSION

Unpeened Material States

The fatigue strength σ_f of both unpeened material states do not differ much, although there are large differences of the appertaining 0.2 % proof stresses and ultimate tensile strengths (see Table 1). The ratio σ_f/R_m amounts to 0.20 (type A) and 0.25 (type B), respectively. These values seems to be rather low when compared to quenched and tempered steels of similiar strength. For example, SAE 4340 steel with ultimate tensile strength of 1375 and 940 N/mm^2 produces ratios σ_f/R_m of 0.25 and 0.32 in push-pull-tests, respectively [10]. However, also in this case the increase of fatigue strength is rather small when compared to the increase of ultimate tensile strength. This finding is commonly explained by the greater notch sensitivity of the harder material states, which makes them more susceptible for surface defects and/or internal defects. Furthermore, the negative effect of unfavourable residual stress states may be stronger than in softer material states, because residual stresses relax less in harder materials when exposed to similiar cyclic loads [11,12]. In the austempered nodular cast iron under investigation, the graphite particles are the most important "internal defects". Accurate measurements of volume changes occuring during tensile loading of ferritic nodular cast iron showed that decohesions at the interface between graphite nodules and the matrix occur at total strains as low as 0.06 % corresponding to a stress of about 100 N/mm^2 [13]. Since this phenomenon is strain controlled and occurs during quasielastic deformation, it can be expected that decohesions at the graphite/matrix interfaces in the higher strength austempered nodular cast irons investigated occur at about the same total strain and stress, respectively. Since all the cyclic loads applied to material states A and B exceed by far these data, it must be concluded that decohesions at the graphite/matrix interfaces - which can be interpreted as microcracks - are present after the first tensile half cycle of each fatigue test. This is an important reason for the lower fatigue strength of austempered nodular cast iron compared to quenched and tempered steel of similiar ultimate tensile strength. The fatigue strength of the material states investigated is determined by their resistance against the spreading and coalescence of microcracks, which lead to the formation of macrocracks, and the materials resistance against macrocrack propagation. Obviously, material states A and B do not differ much in this respect. To understand this, the volume fraction and the stability of retained austenite, which depend on the austempering treatment, have to be regarded. At the relatively high transformation temperature of 380 ^{o}C, the high silicon content of the nodular cast iron investigated prevents carbide precipitation, resulting in a strong enrichment of carbon in the austenitic phase. Consequently, the remaining austenite is chemically stabilized, the reaction becomes very sluggish and finally stops. After cooling to room temperature, a large content of very stable retained austenite is present - 39 vol.-% in the case of material state B. At the relatively low transformation temperature of 300 ^{o}C, the enrichment of carbon in the austenitic phase is less than at 380 ^{o}C. In part, this is due to the higher driving force of the isothermal reaction, which allows for a larger supersaturation in the produced bainitic ferrite. On the other hand, the existence of a metastable eutectoid reaction $\gamma \rightarrow \varepsilon$-carbide + α' at 350 ^{o}C is supposed [14]. Hence, the precipitation of ε-carbide in the bainitic ferrite during isothermal reaction seems to be possible. Consequently, the austenitic phase is less stabilized than at 380 ^{o}C, the reaction can proceed to a larger extend and some transformation of austenite to martensite may occur during cooling from transformation temperature to room temperature, resulting to some extend in a mechanical stabilization of retained austenite. Finally, a smaller amount of less stable retained austenite is present after transformation at 300 ^{o}C compared to transformation at 380 ^{o}C. The similiar fatigue strengths of material states A and B are essentially due to the presence of a large volume fraction of ductile, relatively stable retained austenite in material type B, which has the ability to extensively workharden and to locally transform into martensite at high plastic deformations. The austenite $\rightarrow$ martensite reaction is combined with a local increase in

volume, creating local compressive stresses and locally reducing the effective stress intensity K_{max}. Hence, the propagation of micro- and macrocracks is retarded. This mechanism is much more effective in material state B than in material state A due to the larger volume fraction and stability of the retained austenite, and balances the different strengths of the bainite in both materials.

Shot Peened Material States

A remarkable fact concerning the depth distributions of residual stresses shown in Fig. 1 is the existence of two maxima of compressive stresses. In the case of steels of similiar hardness, one maximum and a continous decrease of residual stresses towards the surface is expected [15]. In the austempered cast irons investigated, the increase of compressive residual stresses towards the surface is caused by the peening induced transformation of retained austenite into martensite. This increase is much stronger in type B than in type A, because twice as much retained austenite is transformed at the surface (see Fig. 4). The transformation is combined with a local volume increase resulting in additional compressive residual stresses near the surface. An upper bound for these stress increments may be estimated if an elastic accomodation in the surrounding bainitic microstructure is assumed. Supposing an isotropic volume increase of 2.1 % [8], the local elastic strain ε becomes 0.7 %, resulting in a mean stress increment

$$\Delta \sigma^{*}(x) = - \Delta RA(x) \cdot E \cdot \varepsilon \,, \qquad (1)$$

where E is Young's modulus. From the depth distribution of retained austenite (see Fig. 3), the transformation induced stress increments may be estimated. As an example, the result of the estimation for type B is given in Fig. 6. If $\Delta\sigma^{*}(x)$ is subtracted from the

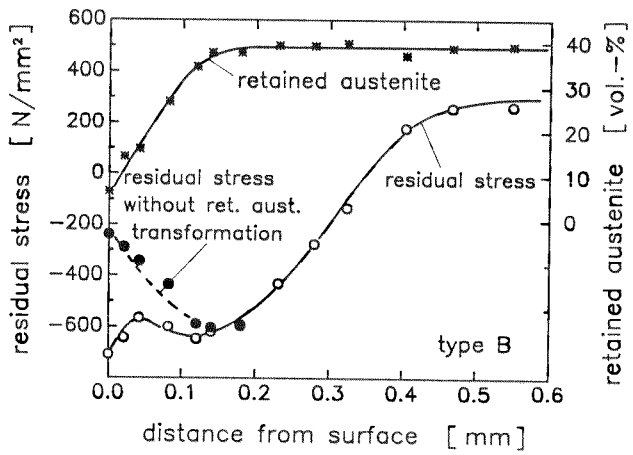

Fig. 6 Residual stress as a function of distance after correction by transformation induced stress increments

measured $\sigma^{rs}(x)$, a depth distribution of residual stresses comparable to that in shot peened steel of similiar hardness is obtained. The amount of residual stresses at the surface, however, seems to be rather low, indicating that the estimated $\Delta\sigma^{*}$-values are too large. Obviously, there is some plastic accomodation of the transformation strains during shot peening.

In relatively soft phases like retained austenite, the plastic deformations caused by shot peening are largest at the surface and become smaller towards the interior of the component or specimen. Fig. 4 shows that the volume fraction of retained austenite transformed to martensite during shot peening is largest at the surface and decreases continuously with increasing distance from the surface. Obviously, the transformation of retained austenite is strain assisted and the amount of martensite produced increases with increasing deformation. This finding corresponds to the high stability of retained austenite in the material states investigated, which excludes stress assisted transformation at room temperature.

In both material states, the half width measured in the bcc phases is generally decreased by shot peening (see Fig. 2). Only at the very surface of material state B, a distinct increase of half width is observed compared with values measured in distances of 0.5 mm or more from the surface. The locus of the minima of half width roughly corresponds with the locus of the maxima of compressive residual stresses. The reduction of half width is caused by the rearrangement of dislocations during plastic deformation in the bainitic ferrite and (in the case of type A) in martensite. The increase of half width towards the surface has two reasons. On the one hand, the amount of peening induced plastic deformation increases towards the surface, possibly resulting in an increasing number of newly produced dislocations. On the other hand, peening induced transformation of retained austenite occurs in a surface layer of 0.3 mm (type A) and 0.2 mm (type B) thickness, respectively. The martensite produced during transformation broadens the interference lines. The volume fraction of retained austenite transformed to martensite comes to 15 % and 33 % at the surfaces of material state A and B, respectively. Therefore, the increase of half width towards the surface is much steeper in material state B than in type A. Consequently, the difference of half width occuring at the surface of shot peened specimens is only 40 % of the difference in the bulk materials.

Contrarily to the measured half width, the hardness continuously increases towards the surface (see Fig. 3). This phenomenon also occurs in shot peened steels of high hardness and is attributed to the influence of compressive residual stresses on the hardness measurement [16]. Concerning the material states investigated, an additional influence arises because the varying content of martensite produced by shot peening may have a stronger effect on the depth distribution of hardness than on that of half width. It is interesting that independent of the distance from surface the hardness of both material states differs by approximately 150 HV 0.5, although more martensite is produced by shot peening near the surface in material state B than in material state A. Obviously, with regard to hardness, the influences of different volume fractions of martensite and different amounts of compressive residual stresses balance each other.

The most remarkable result of the present investigation is the much higher fatigue strength of shot peened material state B compared to shot peened material state A. Neither the unpeened material states nor the depth distributions of residual stresses, half width and hardness produced by shot peening give any obvious reason for this finding. The improvement of the fatigue strength of materials with hardness exceeding 40 HRC by shot peening is commonly attributed to peening induced compressive residual stresses, which are relatively stable during cyclic loading with stress amplitudes corresponding to the fatigue limit [11]. The concept of local fatigue strength has proved useful in describing the influence of shot peening on the fatigue behaviour of steels in different *heat treating states [17,18]. A local fatigue strength* σ_f^{local} *is associated with each* material layer, depending on the fatigue strength of the unpeened material state σ_f and the peening induced compressive residual stresses σ^{rs} as well as increments of hardness HV:

$$\sigma_f^{local} = \sigma_f - m \cdot \sigma^{rs} + n \cdot \Delta HV \ . \qquad (2)$$

The residual stress sensitivity m is generally accepted to be smaller than the mean stress sensitivity, m^*[19]. Hence, m^* could serve as an upper bound for the residual stress sensitivity of the material states investigated. In the following, the Goodman approximation $m^* = \sigma_f/R_m$ is used. From Table 1 and Fig. 5, m^* comes to 0.20 (type A) and 0.25 (type B), respectively. The hardness sensitivity n may be calculated from the changes of hardness and of fatigue strength of unpeened material states A and B ($n = \Delta\sigma_f/\Delta HV$) and come to n = 0.25. This value is somewhat doubtful, because at material states of high hardness like type A, a further increase in hardness may be detrimental and not beneficial to the fatigue strength [10]. It will be shown, however, that the actual value of n is insignificant to the conclusions to be drawn.

In Fig. 7, the local fatigue strength calculated is plotted as a function of distance from surface. At depths exceeding 0.4 mm (type A) or 0.33 mm (type B), the calculated data are smaller than the fatigue strength of the unpeened material state because there are

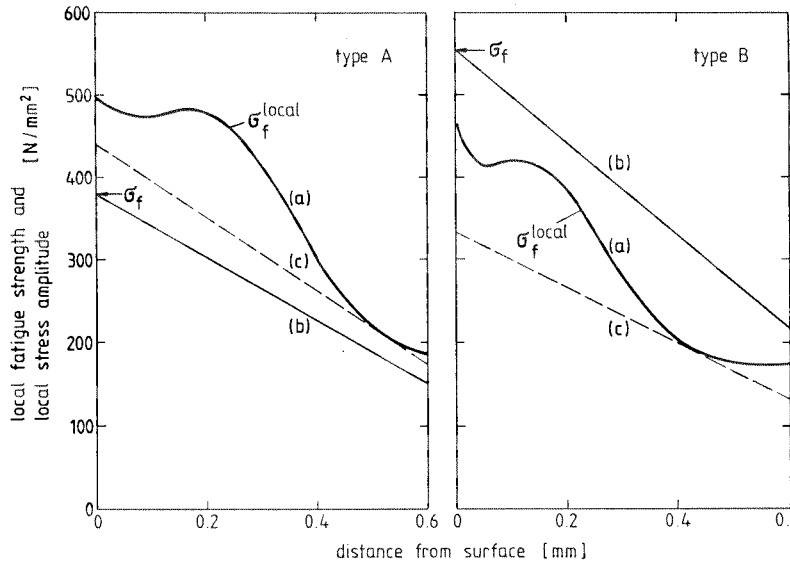

Fig. 7 Local fatigue strength and local stress amplitude in cyclic bending tests as a function of distance from surface

tensile residual stresses (see Fig. 1). The smallest load stress distributions, for which fracture is expected, are plotted as broken lines. They touch the graphs of local fatigue strength 0.52 mm (type A) and 0.42 mm (type B) below the surface. Actually, crack initiation was observed in depths increasing from 0.2 to 0.5 mm with decreasing load stress amplitudes. As hardness is hardly influenced by shot peening at depths exceeding 0.2 mm (see Fig. 3), the value of n is insignificant, as mentioned above. The load stress distributions corresponding to the measured fatigue strength σ_f are plotted as full lines. In the case of material type A, expected and measured load stress distributions differ by 30 N/mm² in the vicinity of the expected crack initiation site, which is not surprising in view of the uncertainty in determining the residual stress sensitivity m. Consequently, the measured fatigue strength σ_f = 385 N/mm² is smaller than the value expected from the broken line, σ_f^* = 440 N/mm². In the case of material state B, however, σ_f = 560 N/mm² is much greater than the expected value, σ_f^* = 335 N/mm² and than the fatigue strength of material type A, although the compressive residual stresses and the hardness of type A are always markedly larger than those of type B. The larger amount of retained austenite transformed to martensite in type B during shot peening also gives no valid explanation, because hardness is still larger at the surface of material state A and there is no peening induced transformation at the observed crack initiation sites (see Fig. 4).

The important fact is that a larger amount of stable austenite is present in material state B compared to material state A. X-ray measurements at the fracture surface of type B showed that 22 to 30 vol.-% retained austenite were transformed to martensite in the vicinity of the crack initiation site, depending on the stress amplitude ranging from 550 to 800 N/mm^2. On the contrary, in material state A 8 to 10 vol.-% retained austenite were transformed, corresponding to stress amplitudes ranging from 400 to 600 N/mm^2. As discussed above, the fatigue strength of the material states investigated is essentially determined by the growth and coalescence of microcracks, which are nucleated at the graphite/matrix interfaces. It is assumed that in material state B this process is hindered to a large extend by the workhardening and the strain assisted transformation of retained austenite, which produces large hydrostatic stress components. This mechanism is much more effective below the surface than at the surface, where only biaxial stress states can exist. Consequently, a large increase of the fatigue strength is produced by shot peening, because it shifts the crack initiation site below the surface. It is interesting in this connexion that the peening induced increase of fatigue strength of other high strength material states without transformable phases is rather low, if the crack initiation site is shifted below the surface. For example, the bending fatigue strength of hardened SAE 1045 steel is only increased from 673 to 736 N/mm^2 by shot peening [12]. This difference may simply be explained by the depth distribution of the loading stresses, resulting in lower stress amplitudes at the crack initiation site below the surface than at the surface. On the contrary, the increase of fatigue strength of material state B in the present investigation is mainly determined by the larger resistance to crack initiation below the surface than at the surface. These findings also explain the large scatter concerning literature data of the fatigue strength of austempered nodular cast iron with large amounts of retained austenite, because any machining which produces compressive residual stresses at the surface and shifts the crack initiation site below the surface will produce a large increase of fatigue strength.

REFERENCES

[1] Johansson, M.: Trans AFS 85 (1977), 117/122
[2] Dorazil, E.; Barta, B.; Crhak, J.; Münsterova, E.: Met. Sci. and Heat Treatm. 20 (1978), 532/535
[3] Löhe, D.; Macherauch, E.: Proc. 8th Int. Conf. Strength of Metals and Alloys (ICSMA 8), Pergamon Press, Oxford (1988), Vol. 2, 1245/1250.
[4] Hauke, W.; Hornung, K.: Härterei-Techn. Mitt. 38 (1983), 72/76
[5] Johansson, Vesanen, A.; Rettig, H.: Antriebstechnik 15 (1976), 593/600
[6] Yoshino, S.: Proc. 2nd Int. Conf. Austempered Ductile Iron. ASME-Gear Research Institute (1986), 337/348
[7] Macherauch, E.; Müller, P.: Z. angew. Physik 13 (1961), 305/312
[8] Bartels, R. J.: Dr.-Ing. Dissertation, Universität Karlsruhe (1987). Fortschritts-Berichte VDI, Reihe 5, Nr. 162, VDI-Verlag Düsseldorf (1989).
[9] Dengel, D.: Z. Werkstofftechnik 6 (1975), 253/261
[10] Eifler, D.: Härterei-Tech. Mitt. 39 (1984), 233/252
[11] Vöhringer, O.: In "Advances in Surface Treatments" (Ed. A. Niku-Lari) Vol. 4. Int. Guidebook on Residual Stresses, Pergamon Press, London (1987), 367/396
[12] Hoffmann, J. E.; Löhe, D.; Macherauch, E.: In "Proc. 3rd Int. Conf. Shot Peening". DGM-Informationsgesellschaft, Oberursel (1987), 631/638
[13] Löhe, D.: Dr.-Ing. Dissertation, Universität Karlsruhe (1980)
[14] Hehemann, R. F.: Proc. ASM-Sem. Phase Transformations. ASM, Metals Park, Ohio (1970), 397/432
[15] Wohlfahrt, H.: In "Residual Stresses and Stress Relaxation", Sagamore Army Materials Res. Conf. Proc. (Ed. E. Kula, V. Weiss). Plenum Press, New York, Vol. 28 (1982), 71/92
[16] Vöhringer, O.: In "Proc. 3rd Int. Conf. Shot Peening". DGM-Informationsgesellschaft, Oberursel (1987), 185/204
[17] Hoffmann, J. E.: Dr.-Ing. Dissertation, Universität Karlsruhe (1984)
[18] Starker, P.; Wohlfahrt, H.; Macherauch, E.: Fatigue of Engineering Materials and Structures 1 (1979), 319/327
[19] Macherauch, E.; Wohlfahrt, H.: In "Ermüdungsverhalten metallischer Werkstoffe" (Ed. D. Munz), DGM-Informationsgesellschaft, Oberursel (1985), 237/283